Weightbearing Computed Tomography Measurements in Progressive Collapsing Foot Deformity: A Contemporary Review

Aly Maher Fayed, MD, MSc[1,2] iD, Matthew Jones, BS[3] iD,
Kepler Alencar Mendes de Carvalho, MD[3,4] iD,
Nacime Salomão Barbachan Mansur, MD, PhD[3,4,5] iD,
and Cesar de Cesar Netto, MD, PhD[3,4] iD

Key points

- Weightbearing computed tomography (WBCT) is less prone to perspective distortion of the lower limb due to lower limb malrotation, operator-dependent bias, and bone superimposition. Additionally, WBCT allows for capture of 2-dimensional (2D) and 3-dimensional (3D) measurements with better interobserver reliability than conventional radiography.
- WBCT's rapid evolution includes continuous refinement of different parameters that help diagnose, classify, evaluate, and appraise treatment options in progressive collapsing foot deformity (PCFD) patients.
- Recently, several WBCT parameters were validated as diagnostic tools with reasonable sensitivity and specificity to differentiate between progressive collapsing foot deformity (PCFD) and normal individuals.
- WBCT could help evaluate different classes of PCFD deformity (class A, B, C, D, and E).
- Foot and ankle offset (FAO) is the most specific parameter to diagnose PCFD, whereas middle facet subluxation (MFS) is the most sensitive.

Introduction

Flatfoot represents a spectrum of deformities affecting joints of the foot and ankle. Early literature described

flatfoot deformity as flattening of the medial arch of the foot.[24] Recently, the development of more advanced imaging techniques has enabled 3-dimensional (3D) analysis of different joints of the foot and ankle, which provides better insight into flatfoot deformity.[32] Recent advances have also led to the development of the concept of progressive collapsing foot deformity (PCFD).[35,38] In 2020, a consensus group proposed PCFD as a new nomenclature associated with a classification system that could better portray the different presentations of flatfoot deformity.[10,38]

WBCT has been a reliable tool when evaluating complex foot and ankle conditions.[33] This has been specifically demonstrated in the setting of PCFD.[11,34] In comparison to

[1]Department of Orthopaedic Surgery, Carver College of Medicine, University of Iowa, Iowa City, IA, USA
[2]Department of Orthopaedics and Traumatology, Tanta University Faculty of Medicine, Tanta, Egypt
[3]Department of Orthopedics and Rehabilitation, Carver College of Medicine, University of Iowa, Iowa City, IA, USA
[4]Department of Orthopaedic Surgery, Division of Foot and Ankle Surgery, Duke University Health System, Morrisville, NC, USA
[5]Department of Orthopaedic Surgery, MedStar Union Memorial Hospital, Baltimore, MD, USA

Corresponding Author:
Cesar de Cesar Netto, MD, PhD, Department of Orthopaedic Surgery, Division of Foot and Ankle Surgery, Duke University Health System, 311 Trent Drive, Box 104002, Durham, NC 27710, USA.
Email: Cesar.netto@duke.edu

conventional plain radiography, WBCT is less prone to perspective distortion of the lower limb because of lower limb malrotation, operator-dependent bias, and bone superimposition.[15] Additionally, it allows for capture of 2-dimensional (2D) and 3D measurements with better interobserver reliability.[9,18,26]

This manuscript aims to summarize key WBCT metrics used in evaluation of PCFD cases, highlighting their clinical utility and relevance to surgical planning.

2D Measurements

The axial plane

This plane is parallel to the horizontal platform with the horizontal edge of the images aligned with the first metatarsal axis.[11]

1. **Talonavicular coverage angle (TNCA):** This is the angle between 2 lines in the talonavicular joint. The first line is drawn across the talar head articular surface, and the second line is drawn across the edges of the articular surface of the proximal navicular (Figure 3).[45] This angle quantifies the amount of forefoot/midfoot abduction (class B PCFD). Lintz et al[34] found that TNCA in PCFD patients, with an average reading of 27.8 degrees (SD 11.9 degrees), was significantly increased relative to the control group, which had an average of 14.2 degrees (SD 6.7 degrees) ($P < .001$). Interobserver reliability was 0.96 (95% CI 0.83-0.96), and intraobserver reliability was 0.97 (95% CI 0.93-0.97). Receiver operating characteristic (ROC) curve analysis in the same study revealed that TNCA threshold value $\geq$25.1 degrees was diagnostic of PCFD with a sensitivity of 60.7% and a specificity of 96.4%.[34] A study performed by de Cesar Netto et al[11] resulted in an average TNCA measurement of 30 degrees (95% CI 27-34) in patients with PCFD. Interobserver reliability was 0.39 (95% CI 0.21-0.40), and intraobserver reliability was 0.88 (95% CI 0.72-0.95). Fuller et al[23] found the average TNCA was 28.67 degrees (SD 8.7 degrees) in patients with PCFD. Interobserver and intraobserver reliabilities were 0.66 and 0.77, respectively.

2. **Talus–first metatarsal angle—axial view (TFMA-A):** This angle results from the intersection of the first metatarsal longitudinal axis and talar axis (the line connecting midpoints of the articular surfaces of the talar head and neck at its narrowest width). It reflects the amount of forefoot/midfoot abduction (class B PCFD).[48] In a study by Fuller et al,[23] the average TFMA-A in PCFD patients was 23.46 degrees (SD 8.87 degrees). Interobserver and intraobserver reliabilities were 0.93 and 0.95, respectively. In another study by Lintz et al,[34] the average TFMA-A in PCFD patients was 16.2 degrees (SD 8.8 degrees). This was significantly increased compared to controls ($P < .001$), who had an average TFMA-A of 7.2 degrees (SD 5.6 degrees). Interobserver reliability was 0.96 (95% CI 0.83-0.96), and intraobserver reliability was 0.97 (95% CI 0.93-0.97). In a different cohort, the average TFMA-A of PCFD patients was 20 degrees (95% CI 17-23). Interobserver reliability was 0.54, and intraobserver reliability was 0.89 (95% CI 0.75-0.96).[11]

The Coronal Plane

This plane is perpendicular to the horizontal platform. The horizontal edges of the images are aligned with a line perpendicular to the bimalleolar axis of the ankle.[11]

1. **Subtalar horizontal angle:** This is an angle between the posterior facet of the talus and the floor (horizontal line) that can be measured at 3 consecutive points across the anteroposterior surface of the posterior facet of the subtalar joint (25% or posterior, 50% or midpoint, and 75% or anterior).[42] In a case-control study, the subtalar horizontal angle was found to be significantly higher in PCFD patients when compared to controls at all levels of the posterior subtalar facet ($P < .001$). The mean subtalar horizontal angle average (which is the average of the measurement at the 3 different points) was found to be 15.3 degrees in PCFD patients and 4.5 degrees in the control group. For the points at 25%, 50%, and 75%, the values were 26.7, 14.8, and 4.3 degrees, respectively, demonstrating that the posterior facet is positioned progressively more and more valgus from anterior, to midpoint and posterior.[43] In a case-control study, there was a significant increase in this angle measurement when compared to the control group: 15.9 degrees (SD 5.7) vs 5.7 degrees (SD 6.7), respectively ($P < .001$).[12] In another cohort of 20 PCFD patients, the mean subtalar horizontal angle at 25% was 25 degrees (95% CI 24-27) with an intraobserver reliability of 0.88 (95% CI 0.71-0.95). At 50%, it was 18 degrees (95% CI 16-20) with an intraobserver reliability of 0.92 (95% CI 0.80-0.97). Finally, at 75%, the mean subtalar horizontal angle was 13 degrees (95% CI 11-15) with an intraobserver reliability of 0.90 (95% CI 0.75-0.96). Interobserver reliabilities were substantial at 25%, 50%, and 75%, with values of 0.68, 0.62, and 0.64, respectively.[11]

2. **Middle facet subluxation (MFS):** This metric represents the percentage of the middle facet of the

talus that is uncovered by the articular surface of the calcaneus (Figure 6).[16] MFS serves as a direct measurement of the amount of peritalar subluxation (PTS) (class D PCFD). de Cesar Netto et al[16] found that the middle facet in PCFD patients demonstrated significantly higher mean joint uncoverage of 45.3% (95% CI 38.5-52.1) vs 4.8% (95% CI 3.2-6.4) in controls (*P* < .0001). Intraobserver reliability was 0.90 (95% CI 0.81-0.95). In another study, a threshold value of MFS >28.7% subluxation had 100% specificity and a sensitivity of 92.8% for diagnosis of PCFD.[34] Barbachan Mansur et al[4] studied 74 symptomatic PCFD patients to evaluate MFS association with foot and ankle offset (FAO), they found that when the MFS was greater than 27.5%, there was an associated increase in mean FAO from 2.4% to 8.0%, which reflected increased mal-alignment severity.

3. **Middle facet incongruence angle:** This angle, which also helps quantify PTS, is measured between the articular surface of the talus and calcaneus at the middle facet.[16] A study found that a threshold of >10.9 degrees for this angle has a very high specificity of 96.4% when used in the diagnosis of PCFD. However, sensitivity of this threshold is 78.5%.[34] In a study by Lintz et al,[34] the angle was found to have an average of 13.3 degrees (SD 5.3) in PCFD patients in comparison to the control group, which had an average angle of 5.6 degrees (SD 2.9) (*P* < .001). Interobserver reliability was 0.7 (95% CI 0.45-0.84), and intraobserver reliability was 0.88 (95% CI 0.82-0.93). In another study,[16] the mean angle in the PCFD patients was 17.3 degrees (95% CI 14.7-19.9) vs 0.3 degrees (95% CI 0.1-0.5) in the control group (*P* < .001). The interobserver reliability, which was 0.93 (95% CI 0.85-0.96), and intraobserver reliability, which was 0.95 (95% CI 0.91-0.98), were almost perfect.

4. **Subtalar inferior-superior facet angle:** This angle is measured between the inferior aspect of the talus at the subtalar joint posterior facet and the superior aspect of the talus at the articular surface of the talar dome.[12] Cody et al[12] found that the mean subtalar inferior-superior facet angle in PCFD patients was 21.2 degrees (SD 6.7), whereas the mean angle in the control group was 10.7 degrees (SD 6.4) (*P* < .001). The authors hypothesized it to be a possible intrinsic inherent risk factor for PCFD, where patients born with a more valgus inclined posterior facet of the subtalar joint would have a higher chance to develop PCFD.

5. **Forefoot arch angle (FAA):** This is the angle between a line connecting the most inferior points of the medial cuneiform with the fifth metatarsal and another line representing the floor (Figure 5).[22] The angle is a good representation of collapse of the medial and transverse arches (class C PCFD).[11] A threshold of <11.3 degrees has a sensitivity of 85.7% and specificity of 82.1% in diagnosing PCFD. Interobserver reliability was 0.95 (95% CI 0.92-0.97), and the intraobserver reliability was 0.97 (95% CI 0.96-0.98).[34] In the same study, the authors found that FAA was significantly lower in patients with PCFD in comparison to control patients. The average FAA in PCFD patients was 5.5 degrees (SD 5.8 degrees) vs 14.8 degrees (SD 4.3 degrees) in controls.[34] This angle showed collapse up to 10 degrees (95% CI 8-13) in PCFD patients on WBCT in comparison to nonweightbearing CT (*P* < .0001).[11]

6. **Hindfoot alignment angle (hindfoot valgus angle [HVA]):** This angle is formed by the intersection of the longitudinal axis of the tibial shaft and the longitudinal axis of the calcaneal tuberosity. It has been used to evaluate the valgus of the hindfoot (class A PCFD).[47] Williamson et al,[47] in radiographic study, found that flatfooted patients had an average HVA of 22.5 degrees (SD 4.9 degrees), whereas control patients had a mean angle of 5.6 degrees (SD 5.4 degrees) (*P* < .001). Interobserver and intraobserver reliabilities were excellent: 0.97 and 0.98, respectively. In normal individuals, HVA is estimated to be 2 to 6 degrees of valgus.[8] However, it was greater than 10 degrees of valgus in patients with PCFD.[41] In a cohort of 20 flexible PCFD patients, the mean HVA was 22.8 degrees (95% CI 20.4-25.3). Interobserver and intraobserver reliabilities were 0.73 and 0.88, respectively.[17]

7. **Hindfoot moment arm (HMA):** This is the apparent moment arm of the hindfoot, which was originally described by Saltzman and El Khoury in 1995 on weightbearing radiographs.[44] The HMA has been recently validated on WBCT. HMA is equal to the distance between the most inferior point of the calcaneus and the distal extension of the tibial anatomical axis at the ground level (Figure 2).[2] It is also a measure of hindfoot valgus (class A PCFD). In a cohort of 21 PCFD patients, the mean HMA was 20.79 mm (95% CI 17.56-24.02).[36] The mean HMA in a cohort of 20 patients with flexible PCFD was 15.1 mm (95% CI 13.4-16.9). Interobserver and intraobserver reliabilities were 0.88 and 0.97, respectively.[17]

8. **Calcaneofibular distance (CFD) and subfibular impingement (SFI):** CFD is the minimum distance between the lateral surface of the calcaneus and the

medial aspect of the distal fibula (Figure 4A) and serves as a surrogate for the presence of SFI, subtalar joint ligament insufficiency, and PTS (class D PCFD).[5,25,28] In one study, the mean CFD was found to be 5 mm (95% CI 4.5-5.5) in PCFD patients.[11] In a another study, it was found that all flexible PCFD patients had no SFI. However, 50% of rigid PCFD patients had SFI ($P < .049$).[29] Other studies reported presence of SFI in 6.6% to 19.4% in PCFD patients.[28,30]

9. **Sinus tarsi impingement (STI):** A decrease in the distance between the lateral process of the talus and the calcaneus at the sinus tarsi indicates presence of sinus tarsi impingement, a common symptomatic representation of PTS (class D PCFD) (Figure 4B). In a cohort of 91 PCFD patients, it was found in 51 patients (56%).[28] In another study, sinus tarsi impingement was found in 84.7% of PCFD patients.[30]

10. **Talar tilt angle (TTA):** TTA is the angle between the articular surface of the talar dome and the articular surface of the distal tibia (Figure 7).[14] It represents a measurement of valgus deformity of the ankle joint (class E PCFD). In a cohort of 60 patients with established valgus hindfoot malalignment, the average talar tilt angle was 5.9 degrees, and the interobserver and intraobserver reliabilities were 0.92 and 0.89, respectively.[7] In a case-control study, an inverse relationship between TTA and MFS was found.[36] The authors have demonstrated that once the ankle joints fall in valgus, the amount of PTS measured by the MFS decreases, hypothetically explained by the fact that the subtalar joint would compensate for the ankle valgus, reducing part of the PTS and repositioning in a less subluxated position.

The Sagittal Plane

This plane is perpendicular to the horizontal platform. The horizontal edges of the images are aligned with the longitudinal axis of the second metatarsal.[11]

1. **Talus–first metatarsal angle (TFMA-S):** This angle is formed at the intersection between the longitudinal axes of the first metatarsal and the talus.[48] It is a measure of foot collapse (class C PCFD). In a retrospective case-control study, the mean talus–first metatarsal angle was significantly higher in PCFD patients when compared to the control group: 22.8 degrees (SD 9.6) vs 8.2 degrees (SD 6.3) ($P < .001$). The interobserver reliability was 0.94 (95% CI 0.49-0.92), and the intraobserver reliability was 0.96 (95% CI 0.79-0.95).[34] According to the same study, when the TFMA-S measures >14.3 degrees, it has a specificity of 85.7% and sensitivity

of 78.5% in identifying PCFD.[34] de Cesar Netto et al[11] reported similar results with a mean TFMA-S of 24 degrees (95% CI 22-26) in PCFD patients. However, the authors reported a relatively lower interobserver reliability of this angle in the sagittal (0.39) and axial planes (0.39), which could be attributed to the fact that the talus and first metatarsal are not collinear in the axial or the sagittal plane. The lower interobserver reliability could also be attributed to difficulty in determining the talar axis, especially with dysplastic tali.

2. **Calcaneal inclination angle (calcaneal pitch angle):** This is the angle formed by the intersection of the floor line and a line connecting the most inferior point of the calcaneal tuberosity with the undersurface edge of the anterior process of the calcaneus.[13] It is also a measure of foot collapse (class C PCFD). In a cohort of 72 symptomatic PCFD patients, the average was 14.15 degrees (SD 4.65 degrees).[23] It is worth noting that this angle did not show significant change in PCFD patients when measured in weightbearing vs nonweightbearing position. The average angle in weightbearing status was 16 degrees (95% CI 15-17), whereas in nonweightbearing images it was 15 degrees (95% CI 14-16, $P = .1446$).[11] In a case-control study, the calcaneal inclination angle in PCFD was 3.2 degrees (SD 5.1 degrees), which was significantly lower when compared to the control group value of 8.2 degrees (SD 4.0 degrees) ($P < .001$).[12]

3. **Medial cuneiform–fifth metatarsal height (medial cuneiform height):** This is defined as the distance between the most inferior aspect of the medial cuneiform and most inferior aspect of the base of the fifth metatarsal.[1,27] It is a measure of foot collapse (class C PCFD). In PCFD patients, it was 4.81 mm (SD 3.6 mm). The interobserver and intraobserver reliabilities were excellent, with values of 0.94 and 0.97, respectively.[23,46]

4. **Medial-cuneiform-to-floor distance:** This distance is measured from the most inferior aspect of the medial cuneiform to the floor level. It represents the medial arch height, another measure of class C PCFD.[1,27] A study by Shakoor et al. resulted in an average medial cuneiform–to–floor distance of 17.8 mm (95% CI 14.3-21.3) in 20 PCFD patients.[46] de Cesar Netto et al[11] found this distance had the most dramatic difference between weightbearing and nonweightbearing status in PCFD patients. The average medial cuneiform–to–floor distance measured for nonweightbearing status patients was 29 mm (95% CI 27-31). For weightbearing status, this metric was 18 mm (95% CI 17-19) ($P < .0001$). Interobserver reliability and intraobserver reliability were both 0.99.
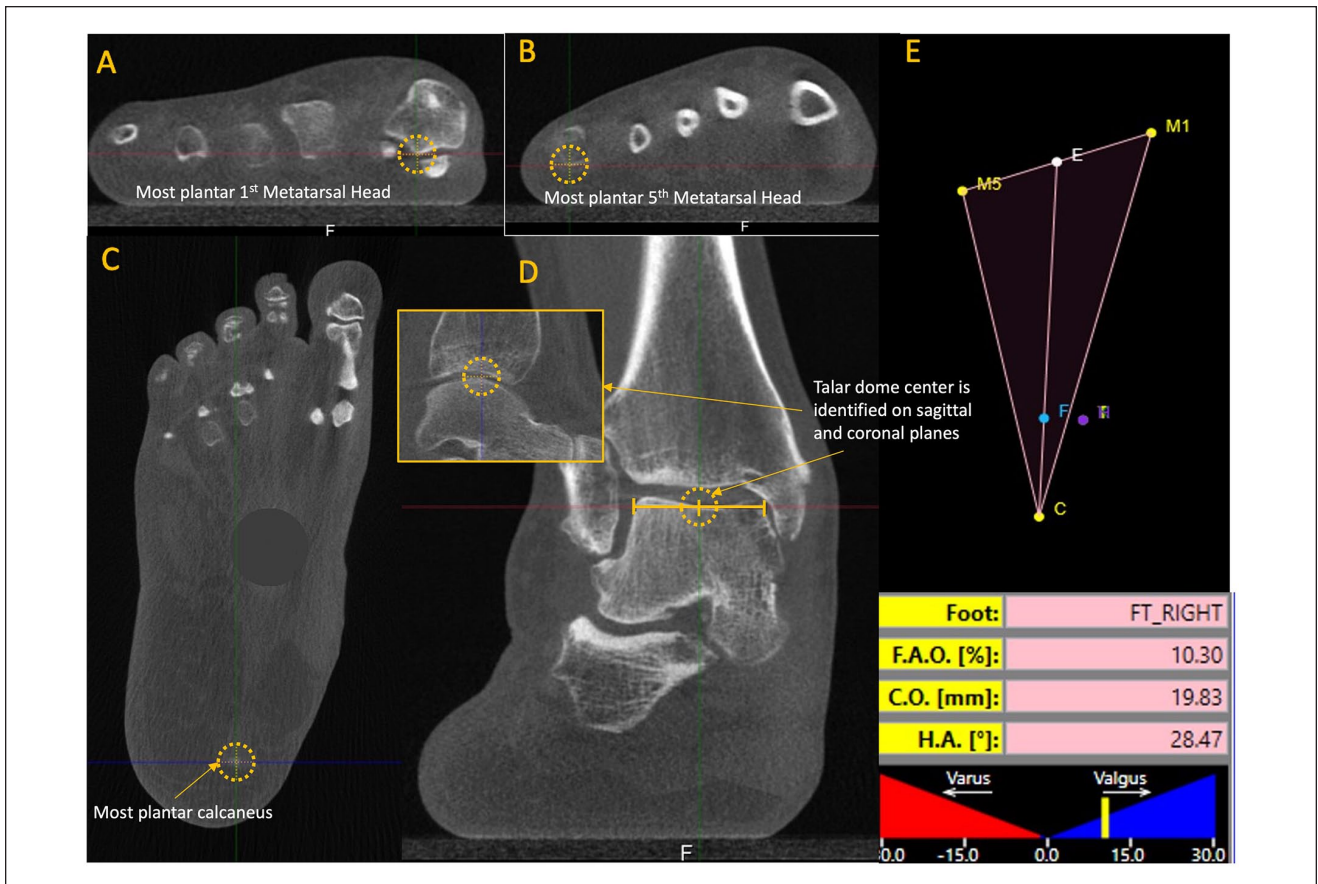
Figure 1. Foot and ankle offset (FAO) semiautomatic measurement. Using the 3 planes (axial, sagittal, and coronal), the most plantar voxel of the first metatarsal, fifth metatarsal, and calcaneus are detected (A, B, and C, respectively). The most proximal as well as central voxel of the talus is detected in both coronal and sagittal images (D). The software calculates the center of foot tripod (M1-M5-C) and the expected position of the ankle joint center (E and F). The displacement percentage in patient's talus position (T) in relation to foot tripod (M1-M5-C-F) is determined as the FAO (E).[34]

5. **Navicular-to-floor distance:** This distance is a class C PCFD surrogate measured from the most inferior aspect of the navicular bone on the coronal view to the floor level.[20] The average of this distance in PCFD patients was 22.7 mm (95% CI 17.9-27.5)[46] and 23 mm (95% CI 22-25)[11] with 0.99 inter- and intraobserver reliabilities.[11]

6. **Cuboid-to-floor distance (C-Fd):** Shakoor et al[46] studied the distance between the floor and the most discernable point on the inferior aspect of the cuboid in patients with PCFD. It is also a measure of foot collapse (class C PCFD).[20] The average cuboid-to-floor distance was 15.7 mm (95% CI 13.3-18.1).[46] de Cesar Netto et al[11] also reported a similar result of 17 mm (95% CI 16-18). The interobserver and intraobserver reliabilities were 0.94 and 0.96, respectively.

3D Measurements

Foot and Ankle Offset (FAO)

FAO is a 3D biometric WBCT measurement and has been demonstrated as a good overall alignment assessment in PCFD and other foot deformities. It quantifies the relationship between the tripod of the foot (first metatarsal, fifth metatarsal, and calcaneus) and the center of the ankle joint (Figure 1).

In other words, the FAO represents the axial offset between the weightbearing centers of the ankle joint and the bisecting line of the foot tripod.[34] Mean FAO was found to be 2.43% (95% CI 2.05-2.82) in the largest reported database of WBCT measurements in patients with various foot and ankle conditions at a single academic institute.[43]

In a study by Lintz et al,[39] the authors found that the mean FAO was 2.3% (SD 2.9, 95% CI 1.5-3.1) in patients

with neutral alignment. In PCFD patients, the FAO average measurement was 11.4% (SD 5.7%, 95% CI 9.6-13.3) ($P < .001$). The interobserver reliability was 0.95 (95% CI 0.88-0.96), and the intraobserver reliability was 0.96 (95% CI 0.94-0.97). In a prospective comparative study by Zhang et al,[49] the authors calculated the mean FAO to be 8.1% (SD 3.7) in patients with PCFD, whereas the control group's mean FAO was 1.2% (SD 2.8%) ($P < .05$). Lintz et al[34] found that FAO and MFS were respectively the most sensitive and specific tools to detect PCFD. Combining FAO measurement at a threshold value >4.6% and MFS >28.7% yielded 100% sensitivity and specificity for identifying PCFD patients. In a group of 21 PCFD patients, a semiautomatic program yielded a mean FAO (%) of 13.32% (SD 4.32%) and a mean FAO (mm) of 19.45 mm (SD 6.68 mm). Fully automatic segmentation yielded a mean FAO (%) of 13.36% (SD 4.43%) and a mean FAO (mm) of 19.52 mm (SD 6.77 mm).[40] There was no significant difference between semiautomated and fully automated FAO measurements.[40]

Distance mapping and coverage mapping. Distance mapping is a state-of-the-art technique to study the relationship and relative positioning between different bones in the foot and ankle. Careful slice-by-slice tracking of all WBCT images can be performed to obtain a 3D reconstruction. To generate distance mapping results, the 3D images need to be meticulously traced along the silhouette of each individual bone. The tracing process can be extensive and needs to be as precise and accurate as possible.[19] Tracing can be done manually or by using certain software packages, which expedites the process. These packages include Mimics Innovation Suite (MIS; Materialise, Leuven, Belgium), which is a fully supported semiautomatic segmentation of any bone structure, and Bonelogic Ortho Foot and Ankle (DIS; Disior, Paragon28, Helsinki, Finland), which is a fully automatic segmentation tool dedicated to foot bones. When 21 PCFD patients underwent assessment of their WBCT imaging using the 2 software packages, there was no statistically significant difference in various measurements between the semiautomatic and the fully automatic methods.[40]

In a case-control study by Dibbern et al, coverage was decreased in the articular regions of the subtalar joint, whereas impingement was increased in the nonarticular regions in PCFD patients. Significant uncoverage occurred only at the middle facet (mean difference = 46.6%, $P < .001$), but not in the anterior or posterior facets. In the same study, sinus tarsi coverage was more frequent in PCFD patients than subfibular impingement. Sinus tarsi coverage was found in 98.0% of PCFD patients ($P < .007$), whereas SFI was found in only 5% of PCFD patients.[19]

Auch et al. performed distance mapping analysis of the distal tibiofibular syndesmosis (DTFS), which was assessed

semiautomatically on axial plane WBCT 1 cm proximal to the tibial plafond. Sixty-two symptomatic PCFD patients were compared with 29 controls. It was found that the FAO had a 6.9% increase in patients with PCFD compared with controls ($P < .001$). Patients with symptomatic PCFD also had increased DTFS in comparison to controls (mean difference = 10.4 mm², $P = .026$).[3]

A case-control study by Behrens et al[6] assessed potential differences in Chopart joint coverage (talonavicular and calcaneocuboid joints coverage) between PCFD patients and controls. In PCFD patients, talar head coverage decreased in both plantar medial and dorsal medial regions (–79%, $P = .003$, and –77%, $P = .00004$, respectively). Calcaneocuboid coverage decreased in plantar and medial regions as well (–11.9%, $P = .006$, and –8.7%, $P = .037$, respectively).

WBCT and PCFD Classification

The WBCT parameters addressed in this article can provide quantification that is useful in the context of the PCFD classification system. According to the consensus meeting, PCFD could be classified into 2 stages (stage I = flexible, stage II = rigid) and 1 or more of 5 classes (class A = hindfoot valgus deformity, class B = midfoot/forefoot abduction deformity, class C = forefoot varus deformity/medial column instability, class D = peritalar subluxation or dislocation, and class E = ankle instability).[21,38]

Although there is no global consensus on cutoff values for several foot and ankle measurements on WBCT, the metrics and associated reference values reported in this study could be useful reference parameters when assessing foot and ankle deformities. In the authors' opinion, WBCT is an integral and crucial tool to evaluate and treat PCFD. The following table displays each class in the PCFD consensus classification coupled with corresponding WBCT parameters (Table 1).

Senior Author's Approach

In our practice, WBCT is routinely obtained for PCFD patients preoperatively and postoperatively at 3, 6, and 12 months, and then annually after that. Initially, we establish the diagnosis of PCFD when FAO is more than 4.6% and MFS is greater than 28.7%. Attention is also given to the presence of sinus tarsi impingement and SFI. Further, WBCT can help characterize deformity classes and help planning therapeutic approaches for them. For class A, we commonly use the HMA, which will also provide us with a notion on how much the calcaneus would need to be displaced to regain a position under the tibial axis. The TNCA is the metric we use to determine class B, using 40 degrees as a threshold to consider performing a lateral column lengthening procedure. Medial column instability and forefoot varus, class C elements, are established by the

Table 1. PCFD Consensus Classification Coupled With Corresponding WBCT Parameters.

Class	Clinical Correlation	WBCT Parameters
Class A	Valgus hindfoot deformity	• FAO >4.6% (sensitivity 89.2%, specificity 100%).[34] (Figure 1) • HVA: normal, 5.6 degrees (SD 5.4); PCFD, 22.5 degrees (SD 4.9).[4] • HMA: normal, ±8.8 mm; PCFD, 20.79 mm (95% CI 17.56-24.02).[36] (Figure 2)
Class B	Abduction deformity midfoot / forefoot	• TNCA > 25.1 degrees (sensitivity 60.7%, specificity 96.4%).[34] (Figure 3) • Evidence of sinus tarsi impingement.[30] (Figure 4)
Class C	Forefoot varus deformity / Medial column instability	• FAA < 11.3 degrees (sensitivity 85.7%, specificity 82.1%).[34] (Figure 5) • TFMA-S >14.3 degrees (sensitivity 78.5%, specificity 85.7%).[34]
Class D	Peritalar subluxation / dislocation	• MFS >28.7% (sensitivity 100%, specificity 92.8%).[34] (Figure 6) • Evidence of subfibular impingement.[30] (Figure 4)
Class E	Ankle instability	• TTA: normal, <2 degrees[31]; PCFD, 17.10 degrees (95% CI 14.75-19.46).[36,37] (Figure 7)

Abbreviations: FAA, forefoot arch angle; FAO, foot and ankle offset; HMA, hindfoot moment arm; HVA, hindfoot valgus angle; MFS, middle facet subluxation; PCFD, progressive collapsing foot deformity; TFMA-S, talus–first metatarsal angle–sagittal; TNCA, talonavicular coverage angle, degrees; TTA, talar tilt angle; WBCT, weightbearing computed tomography.
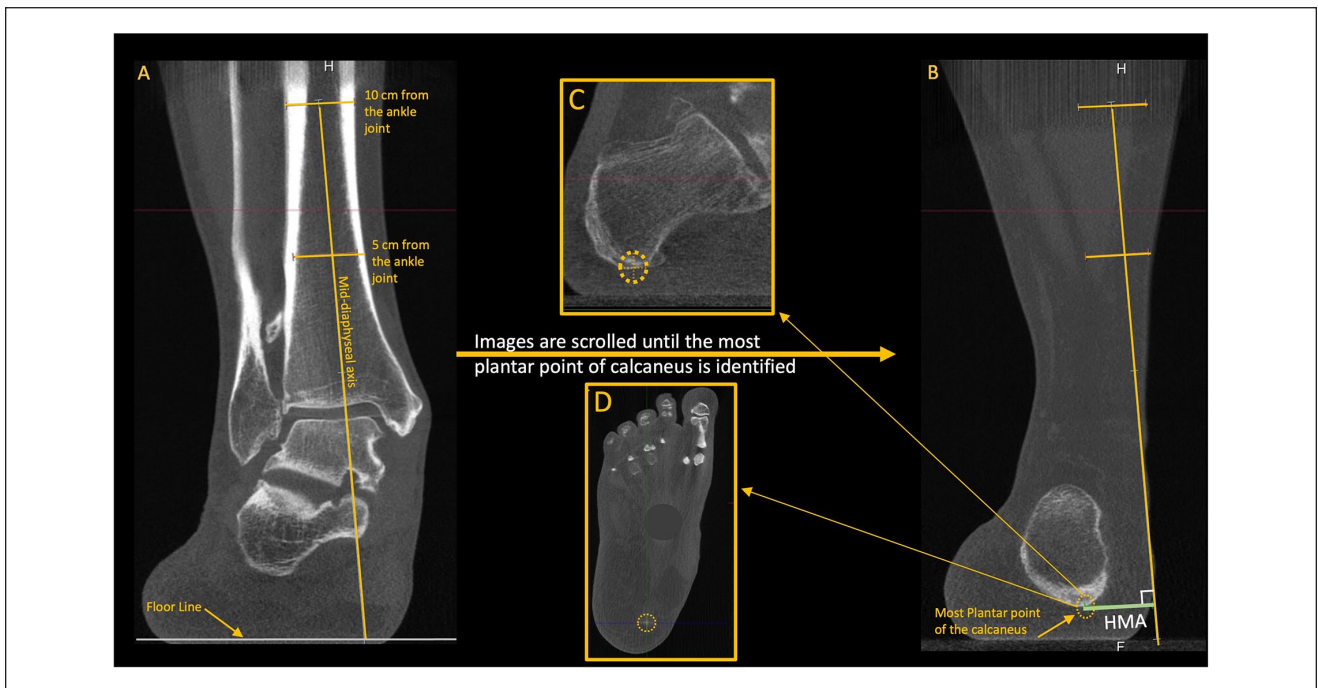

Figure 2. Hindfoot moment arm (HMA). (A) Using the coronal plane, 2 mid-diaphyseal lines are drawn at 5 and 10 cm proximal to the ankle joint to determine the anatomical axis of the tibia. (B) The axis line is then extended inferiorly, crossing the floor line. (B, C, and D) The HMA is determined by the distance between the anatomical tibial line and the most inferior voxel of the calcaneus (confirmed on all planes).[36]

presence of gapping at the TMT or NC joint as well as using the TFMA and the FFA. An overall perception where the instability is present (TMT, NC, TN or all medial column) can help decide where and how to address a class C. Presence of class D and the presence of significant PTS and subfibular impingement have an influence toward a possible subtalar fusion. Ankle valgus tilting and class E are determined by the TTA with implications on the need for a deltoid ligament reconstruction (or a supramalleolar osteotomy) in flexible cases or a total ankle replacement (or an ankle fusion in very selected

cases) in rigid deformities. Moreover, FAO and MFS, as well as distance and coverage maps, are normally used to assess the obtained correction on the postoperative period, as well to help establish recurrence and the necessity for further treatment.

In a flexible condition, that is, 1A, 1B, 1C, 1D, or 1E, our surgical approach usually starts with endoscopic gastrocnemius recession and peroneus brevis transfer to peroneus longus proximal to the superior peroneal retinaculum to decrease deforming forces. Medial displacement calcaneal osteotomy is performed to address flexible hindfoot valgus deformity

Figure 3. Talonavicular coverage angle (TNCA). On the axial view, (A) Marking medial and lateral edges of the proximal navicular articular surface. (B) Marking medial and lateral edges of the talar head articular surface. (C) Full proximal navicular and talar head articular surfaces highlighted. (D) Talonavicular Coverage Angle marked, with lines connecting medial and lateral edges of the proximal navicular and talar head articular surfaces.[34]
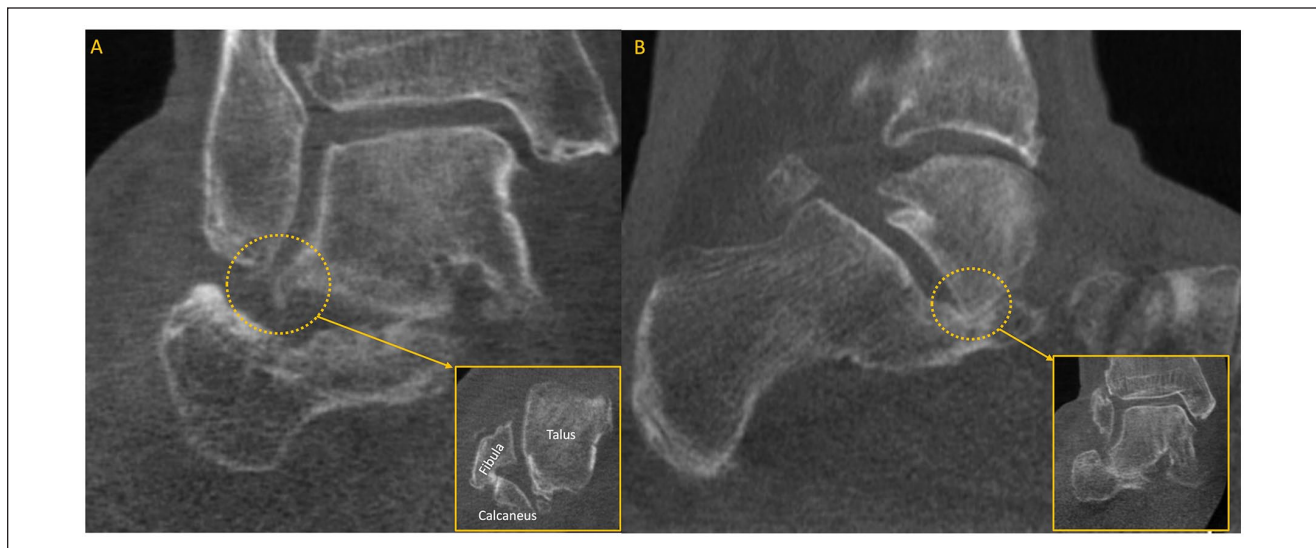

Figure 4. (A) Subfibular impingement. Coronal image shows direct abutment of the talus against the fibular as well as decreased space between the fibular and calcaneus, which is also confirmed on the axial view. (B) Sinus tarsi impingement. Sagittal view shows direct bony impingement at the sinus tarsi between the lateral talus and calcaneus, which is also confirmed on the coronal image.[30]

(class A PCFD). If there is significant collapse of the longitudinal arch (class C PCFD), assessed by increased TFMA-S and decreased FAA, a Cotton osteotomy is considered. If there is need for pronounced correction or there is objective WBCT evidence of first tarsometatarsal joint instability (plantar gapping), our preference is for a modified Lapidus procedure using a plantarflexion bone-block allograft wedge (LapiCotton) to restore the medial longitudinal arch and help reestablish the foot tripod. Usually, forefoot abduction (class B PCFD) is restored after medial displacement calcaneal osteotomy and first ray plantarflexion procedures are performed. If no complete correction is achieved, usually assessed by the TNCA with simulated fluoroscopic imaging, a lateral column lengthening (LCL) would be considered. After bone realignment, if needed, a medial approach to the ankle and midfoot is performed, and reconstruction of the superficial and anterior
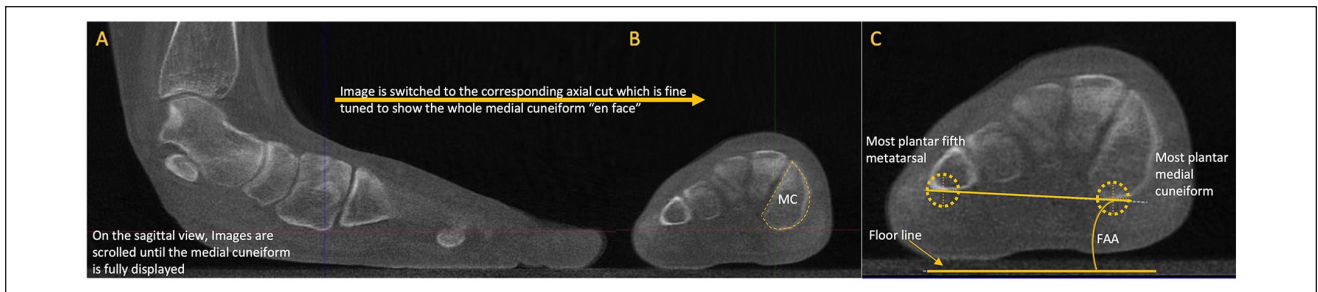
Figure 5. Forefoot arch angle (FAA). Using the sagittal and axial images, the medial cuneiform (MC) is identified, and the axial cut that shows the whole length of the MC is chosen for measurements. The FAA is then measured between 2 lines: one tangential to the already established most plantar aspect of the medial cuneiform and the most plantar voxel of the fifth metatarsal, and the floor line.[34] (A) Cross-section of the Weight-bearing CT imaging is brought to the distal aspect of the medial cuneiform, just proximal to the plantar aspect of the first tarsometatarsal joint line. (B) The corresponding coronal plane image is utilized to calculate the Forefoot Arch Angle, and represents the first full image of the entire medial cuneiform in the coronal plane. (C) The Forefoot Arch Angle is measured as the angulation between a line connecting the lowest point of both the medial cuneiform and fifth metatarsal and the floor line.
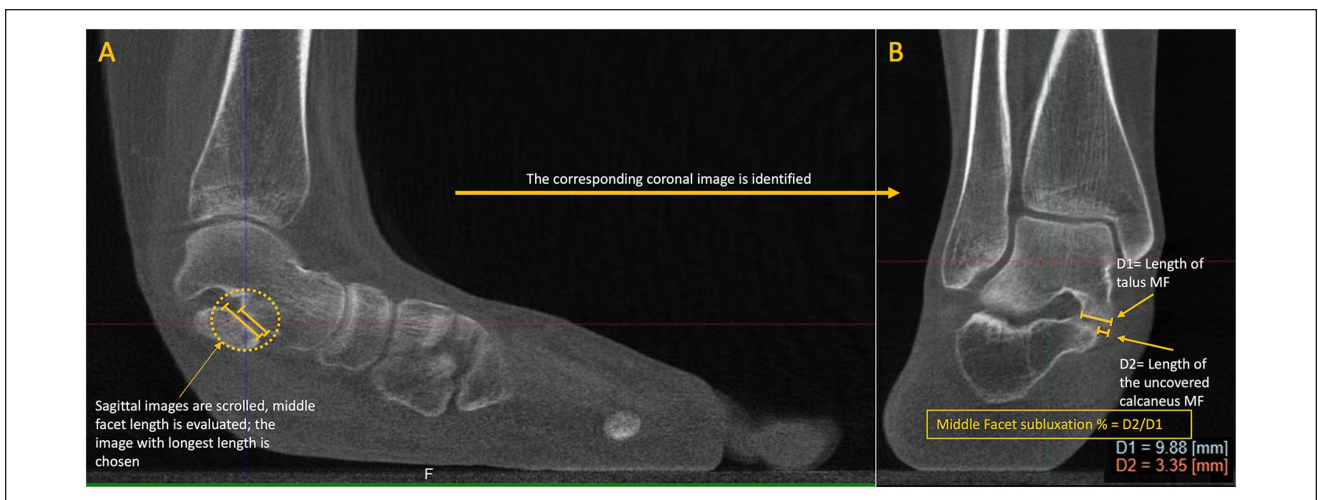

Figure 6. Middle facet subluxation percentage (MFS%). The sagittal view is meticulously evaluated to detect the cut that shows the middle facet perfectly with the longest length, and then the coronal view is evaluated at the same point. The length of the middle facet of the talus is measured (D1). The distance between the most lateral aspect of the calcaneus to the most lateral aspect of the middle facet of the talus is measured as well (D2). MFS% = D2/D1.[34] (A) The longitudinal length of the middle facet of the subtalar joint in the talus and calcaneus is marked. A cross-section of the weight-bearing CT imaging is brought to the anteroposterior midpoint of the middle facet in the talus. (B) The corresponding coronal plane image of the middle facet of the subtalar joint is depicted, with the measurement of middle facet subluxation being highlighted as the fraction between the uncovered distance and the mediolateral distance of the middle facet articular surface in the talus.

deep deltoid is performed using hamstring allograft or commercial suture tape/internal brace. Through the same approach, evaluation of the spring ligament and posterior tibial tendon are completed, which can lead to either a tissue debridement, reconstruction, or flexor digitorum longus tendon transfer.

Conclusion

WBCT is a powerful tool for evaluation of all aspects of PCFD. FAO is the most specific parameter to diagnose PCFD, whereas MFS is the most sensitive. Increased use of WBCT, as well as rapidly evolving 3D technology, will help refine different metrics. Pretreatment and posttreatment evaluation using the described techniques might offer surgeons and patients a more precise judgment of PCFD and its correction, potentially leading to better patient care.
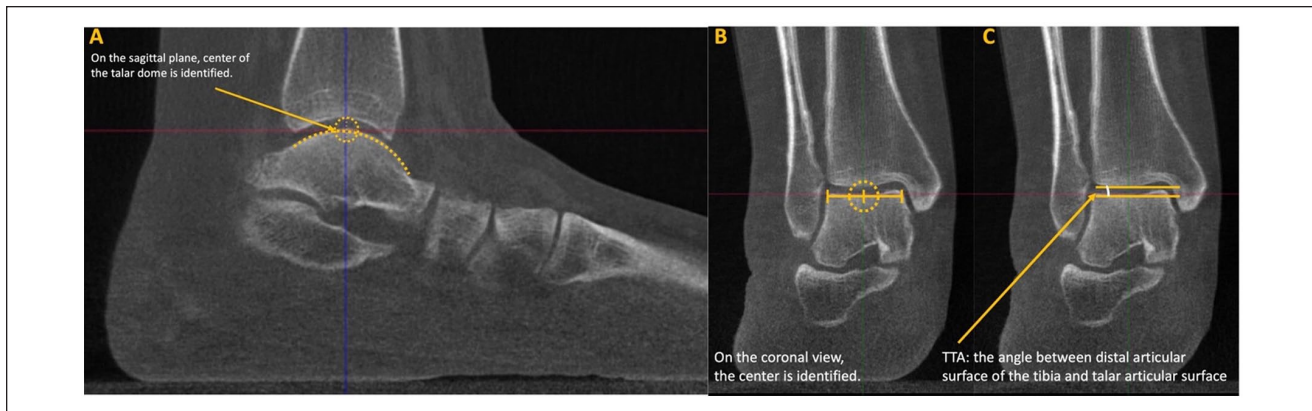
Ethical Approval

Figure 7. Talar tilt angle (TTA). On the sagittal view, the center of the talus is set, and the view is changed to the corresponding coronal plane, where the talus center is also detected. The center of the talus is again set in the sagittal plane (usually coincident with the tibia), the view is changed to coronal, and the tangential line to the superior talar surface is established. The talar tilt angle is measured between 2 lines drawn tangential to the articular surfaces of the distal tibia and talus.[31,36] (A) Cross-section of the Weight-bearing CT imaging is brought to the apex of the talar dome in the sagittal plane. (B) Cross-section of the Weight-bearing CT imaging is also brought to the mediolateral midpoint of the talar dome in the coronal plane. (C) Talar tilt angle is highlighted as the angulation between a tangent line to the talar dome articular surface and one tangent to the distal tibia articular surface.

ORCID iDs

Aly Maher Fayed, MD, MSc, (iD) https://orcid.org/0000-0002-3905-9662
Matthew Jones, BS, (iD) https://orcid.org/0000-0003-0773-7286
Kepler Alencar Mendes de Carvalho, MD, (iD) https://orcid.org/0000-0003-1082-6490
Nacime Salomão Barbachan Mansur, MD, PhD, (iD) https://orcid.org/0000-0003-1067-727X
Cesar de Cesar Netto, MD, PhD, (iD) https://orcid.org/0000-0001-6037-0685

References

1. Arangio GA, Wasser T, Rogman A. Radiographic comparison of standing medial cuneiform arch height in adults with and without acquired flatfoot deformity. *Foot Ankle Int*. 2006;27(8):636-638.

2. Arena CB, Sripanich Y, Leake R, Saltzman CL, Barg A. Assessment of hindfoot alignment comparing weightbearing radiography to weightbearing computed tomography. *Foot Ankle Int*. 2021;42(11):1482-1490. doi: 10.1177/10711007211014171

3. Auch E, Barbachan Mansur NS, Alexandre Alves T, et al. Distal tibiofibular syndesmotic widening in progressive collapsing foot deformity. *Foot Ankle Int*. 2021;42(6):768-775. doi:10.1177/1071100720982907

4. Barbachan Mansur NS, Lalevee M, Maly C, et al. Association between middle facet subluxation and foot and ankle offset in progressive collapsing foot deformity. *Foot Ankle Int*. 2022;43(1):96-100. doi:10.1177/10711007211040820

5. Barg A, Bailey T, Richter M, et al. Weightbearing computed tomography of the foot and ankle: emerging technology topical review. *Foot Ankle Int*. 2018;39(3):376-386. doi:10.1177/1071100717740330

6. Behrens A, Dibbern K, Lalevée M, et al. Coverage maps demonstrate 3D Chopart joint subluxation in weightbearing CT of progressive collapsing foot deformity. *Sci Rep*. 2022;12(1):19367. doi:10.1038/s41598-022-23638-3

7. Burssens A, Peeters J, Buedts K, Victor J, Vandeputte G. Measuring hindfoot alignment in weight bearing CT: a novel clinical relevant measurement method. *Foot Ankle Surg*. 2016;22(4):233-238. doi:10.1016/j.fas.2015.10.002

8. Burssens A, Vermue H, Barg A, Krähenbühl N, Victor J, Buedts K. Templating of syndesmotic ankle lesions by use of 3D analysis in weightbearing and nonweightbearing CT. *Foot Ankle Int*. 2018;39(12):1487-1496. doi:10.1177/1071100718791834

9. Carrino JA, Al Muhit A, Zbijewski W, et al. Dedicated cone-beam CT system for extremity imaging. *Radiology*. 2014;270(3):816-824. doi:10.1148/radiol.13130225

10. Cody EA, Williamson ER, Burket JC, Deland JT, Ellis SJ. Correlation of talar anatomy and subtalar joint alignment

on weightbearing computed tomography with radiographic flatfoot parameters. *Foot Ankle Int*. 2016;37(8):874-881. doi:10.1177/1071100716646629

11. Coughlin MJ, Kaz A. Correlation of Harris mats, physical exam, pictures, and radiographic measurements in adult flatfoot deformity. *Foot Ankle Int*. 2009;30(7):604-612.

12. Cox JS, Hewes TF. "Normal" talar tilt angle. *Clin Orthop Relat Res*. 1979(140):37-41.

13. Dagneaux L, Moroney P, Maestro M. Reliability of hindfoot alignment measurements from standard radiographs using the methods of Meary and Saltzman. *Foot Ankle Surg*. 2019;25(2):237-241. doi:10.1016/j.fas.2017.10.018

14. de Cesar Netto C, Myerson MS, Day J, et al. Consensus for the use of weightbearing CT in the assessment of progressive collapsing foot deformity. *Foot Ankle Int*. 2020;41(10):1277-1282. doi:10.1177/1071100720950734

15. de Cesar Netto C, Schon LC, Thawait GK, et al. Flexible adult acquired flatfoot deformity: comparison between weight-bearing and non-weight-bearing measurements using cone-beam computed tomography. *J Bone Joint Surg Am*. 2017;99(18):e98. doi:10.2106/JBJS.16.01366

16. de Cesar Netto C, Godoy-Santos AL, Saito GH, et al. Subluxation of the middle facet of the subtalar joint as a marker of peritalar subluxation in adult acquired flatfoot deformity: a case-control study. *J Bone Joint Surg Am*. 2019;101(20):1838-1844. doi:10.2106/JBJS.19.00073

17. de Cesar Netto C, Shakoor D, Roberts L, et al. Hindfoot alignment of adult acquired flatfoot deformity: a comparison of clinical assessment and weightbearing cone beam CT examinations. *Foot Ankle Surg*. 2019;25(6):790-797. doi:10.1016/j.fas.2018.10.008

18. Demehri S, Muhit A, Zbijewski W, et al. Assessment of image quality in soft tissue and bone visualization tasks for a dedicated extremity cone-beam CT system. *Eur Radiol*. 2015;25(6):1742-1751. doi:10.1007/s00330-014-3546-6

19. Dibbern KN, Li S, Vivtcharenko V, et al. Three-dimensional distance and coverage maps in the assessment of peritalar subluxation in progressive collapsing foot deformity. *Foot Ankle Int*. 2021;42(6):757-767. doi:10.1177/1071100720983227

20. Ellis SJ, Deyer T, Williams BR, et al. Assessment of lateral hindfoot pain in acquired flatfoot deformity using weightbearing multiplanar imaging. *Foot Ankle Int*. 2010; 31(5):361-371.

21. Fayed A, Mallavarapu V, Schmidt E, et al. Deformities influencing different classes in progressive collapsing foot. *Iowa Orthop J*. 2023;43(2):8.

22. Ferri M, Scharfenberger AV, Goplen G, Daniels TR, Pearce D. Weightbearing CT scan of severe flexible pes planus deformities. *Foot Ankle Int*. 2008;29(2):199-204.

23. Fuller RM, Kim J, An TW, et al. Assessment of flatfoot deformity using digitally reconstructed radiographs: reliability and comparison to conventional radiographs. *Foot Ankle Int*. 2022;43(7):983-993. doi:10.1177/10711007221089260

24. Harris RI, Beath T. Hypermobile flat-foot with short tendo achillis. *J Bone Joint Surg Am*. 1948;30A(1):116-140. doi:10.2106/00004623-194830010-00013

25. Hirschmann A, Pfirrmann CWA, Klammer G, Espinosa N, Buck FM. Upright cone CT of the hindfoot: comparison of the non-weight-bearing with the upright weight-bearing position. *Eur Radiol*. 2014;24(3):553-558. doi:10.1007/s00330-013-3028-2

26. Holbrook HS, Bowers AF, Mahmoud K, Kelly DM. Weight-bearing computed tomography of the foot and ankle in the pediatric population. *J Pediatr Orthop*. 2022;42(6):321-326.

27. Iossi M, Johnson JE, McCormick JJ, Klein SE. Short-term radiographic analysis of operative correction of adult acquired flatfoot deformity. *Foot Ankle Int*. 2013;34(6):781-791.

28. Kim J, Rajan L, Fuller R, et al. Radiographic cutoff values for predicting lateral bony impingement in progressive collapsing foot deformity. *Foot Ankle Int*. 2022;43(9):1219-1226. doi:10.1177/10711007221099010

29. Krähenbühl N, Kvarda P, Susdorf R, et al. Assessment of progressive collapsing foot deformity using semiautomated 3D measurements derived from weightbearing CT scans. *Foot Ankle Int*. 2022;43(3):363-370. doi:10.1177/10711007211049754

30. Lalevée M, Barbachan Mansur NS, Rojas EO, et al. Prevalence and pattern of lateral impingements in the progressive collapsing foot deformity. *Arch Orthop Trauma Surg*. 2023;143(1):161-168. doi:10.1007/s00402-021-04015-7

31. Leith JM, McConkey JP, Li D, Masri B. Valgus stress radiography in normal ankles. *Foot Ankle Int*. 1997;18(10):654-657. doi:10.1177/107110079701801010

32. Li S, Zhu M, Gu W, et al. Diagnostic accuracy of the progressive collapsing foot deformity (PCFD) classification. *Foot Ankle Int*. 2022;43(6):800-809. doi:10.1177/10711007221078000

33. Lintz F, Beaudet P, Richardi G, Brilhault J. Weight-bearing CT in foot and ankle pathology. *Orthop Traumatol Surg Res*. 2021;107(1s):102772. doi:10.1016/j.otsr.2020.102772

34. Lintz F, Bernasconi A, Li S, et al. Diagnostic accuracy of measurements in progressive collapsing foot deformity using weight bearing computed tomography: a matched case-control study. *Foot Ankle Surg*. 2022;28(7):912-918. doi:10.1016/j.fas.2021.12.012

35. Lintz F, de Cesar Netto C, Barg A, Burssens A, Richter M. Weight-bearing cone beam CT scans in the foot and ankle. *EFORT Open Rev*. 2018;3(5):278-286. doi:10.1302/2058-5241.3.170066

36. Mansur NS, Lalevée M, Vivtcharenko V, et al. Predictors of deformity in patients with progressive collapsing foot deformity and valgus of the ankle. *Foot Ankle Orthop*. 2022; 7(2):2473011421S00538. doi:10.1177/2473011421s00538

37. Mansur NSB, Lalevee M, Shamrock A, Lintz F, de Carvalho KAM, de Cesar Netto C. Decreased peritalar subluxation in progressive collapsing foot deformity with ankle valgus tilting. *JB JS Open Access*. 2023;8(4):e23.00025.

38. Myerson MS, Thordarson DB, Johnson JE, et al. Classification and nomenclature: progressive collapsing foot deformity. *Foot Ankle Int*. 2020;41(10):1271-1276. doi:10.1177/1071100720950722

39. Lintz F, Welck M, Bernasconi A, Thornton J, Cullen NP, Singh D, et al. 3D Biometrics for Hindfoot Alignment Using Weightbearing CT. *Foot Ankle Int*. 2017;38:684-689.

40. Ortolani M, Leardini A, Pavani C, et al. Angular and linear measurements of adult flexible flatfoot via weight-bearing CT scans and 3D bone reconstruction tools. *Sci Rep*. 2021;11(1):16139. doi:10.1038/s41598-021-95708-x

41. Pilania K, Jankharia B, Monoot P. Role of the weight-bearing cone-beam CT in evaluation of flatfoot deformity. *Indian J Radiol Imaging*. 2019;29(4):364-371. doi:10.4103/ijri.IJRI_288_19

42. Probasco W, Haleem AM, Yu J, Sangeorzan BJ, Deland JT, Ellis SJ. Assessment of coronal plane subtalar joint alignment in peritalar subluxation via weight-bearing multiplanar imaging. *Foot Ankle Int*. 2015;36(3):302-309. doi:10.1177/1071100714557861

43. Rojas EO, Barbachan Mansur NS, Dibbern K, et al. Weightbearing computed tomography for assessment of foot and ankle deformities: the Iowa experience. *Iowa Orthop J*. 2021;41(1):111-119.

44. Saltzman CL, El-Khoury GY. The hindfoot alignment view. *Foot Ankle Int*. 1995;16(9):572-576. doi:10.1177/107110079501600911

45. Sangeorzan BJ, Mosca V, Hansen ST. Effect of calcaneal lengthening on relationships among the hindfoot, midfoot, and forefoot. *Foot Ankle*. 1993;14(3):136-141. doi:10.1177/107110079301400305

46. Shakoor D, de Cesar Netto C, Thawait GK, et al. Weight-bearing radiographs and cone-beam computed tomography examinations in adult acquired flatfoot deformity. *Foot Ankle Surg*. 2021;27(2):201-206. doi:10.1016/j.fas.2020.04.011

47. Williamson ERC, Chan JY, Burket JC, Deland JT, Ellis SJ. New radiographic parameter assessing hindfoot alignment in stage II adult-acquired flatfoot deformity. *Foot Ankle Int*. 2015;36(4):417-423. doi:10.1177/1071100714558846

48. Younger AS, Sawatzky B, Dryden P. Radiographic assessment of adult flatfoot. *Foot Ankle Int*. 2005;26(10):820-825. doi:10.1177/107110070502601006

49. Zhang JZ, Lintz F, Bernasconi A, Weight Bearing CTISG, Zhang S. 3D biometrics for hindfoot alignment using weight-bearing computed tomography. *Foot Ankle Int*. 2019;40(6):720-726. doi:10.1177/1071100719835492